

## Absence of Dp71 in mdx3cv mouse spermatozoa alters flagellar morphology and the distribution of ion channels and nNOS

Enrique O. Hernández-González<sup>1,\*</sup>, Dominique Mornet<sup>2</sup>, Alvaro Rendon<sup>3</sup> and Dalila Martínez-Rojas<sup>4</sup>

<sup>1</sup>Departamentos de 1Biología Celular y 4Fisiología, Biofísica y Neurociencias, CINVESTAV. Apdo. postal 14740, 07000 México, D.F., México

<sup>2</sup>INSERM U-128. Groupe Muscles et Pathologies, Institut Bousson-Bertrand, 778 rue de la Croix Verte, 34196 Montpellier CEDEX 5, France

<sup>3</sup>INSERM U-592, Lab. de Physiopathologie Cellulaire et Moléculaire de la Rétine, Hôpital Saint-Antoine, 184 rue du Faubourg Saint-Antoine, 75571 Paris CEDEX 5, France

\*Author for correspondence (e-mail: eoton@cell.cinvestav.mx)

### Summary

In muscle, the absence of dystrophin alters the dystrophin associated protein complex (DAPC), which is involved in the clustering and anchoring of signaling proteins and ion and water channels. Here we show that mice spermatozoa express only dystrophin Dp71 and utrophin Up71. The purpose of this study was to explore the effect of the absence of Dp71 on the morphology and membrane distribution of members of the DAPC, ion channels and signaling proteins of spermatozoa obtained from dystrophic mutant mdx3cv mice. Our work indicates that although the absence of Dp71 results in a dramatic decrease in  $\beta$ -dystroglycan, it induces membrane redistribution and an increase in the total level of  $\alpha$ -syntrophin, voltage dependent Na<sup>+</sup> ( $\mu$ 1) and K<sup>+</sup> (Kv1.1) channels and neural nitric oxide synthase (nNOS). The short utrophin (Up71) was upregulated and redistributed in the spermatozoa of mdx3cv mice. A significant increase in abnormal flagella morphology was observed in the absence of Dp71, which was partially corrected when the plasma membrane was eliminated by detergent treatment. Our observations point to a new phenotype associated with the absence of Dp71. Abnormal flagellar structure and altered distribution of ion channels and signaling proteins may be responsible for the fertility problems of mdx3cv mice.

**Key words:** Duchenne muscular dystrophy, Cytoskeleton, Motility, Syntrophin-associated proteins, Utrophin upregulation

## Introduction

Dystrophin is a member of the protein family encoded by the Duchenne muscular dystrophy (DMD) gene, which is expressed in muscular and non-muscular tissues. The DMD gene has internal promoters (Winder, 1997) that encode short dystrophin products of 260 kDa (Dp260), 140 kDa (Dp140), 116 kDa (Dp116) and 71 kDa (Dp71). Full-length dystrophin and all dystrophin proteins (Dps) are expressed in neural tissue (Blake et al., 2001) and Dp71 is widely distributed in nonmuscle tissues (Lederfein et al., 1993). In addition, by alternative splicing of exons 71-74 and/or 78, several isoforms may be generated (Austin et al., 2000). We have shown the expression of Dp71 in brain subcellular fractions (Chávez et al., 2000) and in spermatozoa (Hernández-González et al., 2001). Dystrophin links cytoskeletal actin to the extracellular matrix via a dystrophin glycoprotein complex composed of dystrophin and dystrophin-associated proteins (DAPs) (Ibraghimov-Beskrovnaya et al., 1992) and builds the DAPC, which is composed of  $\beta$ -dystroglycan, sarcoglycans, dystrobrevins and syntrophins (Ervasti and Campbell, 1993).

At the neuromuscular junction and in non-muscular tissues, utrophin, a dystrophin-related protein (DRP), is also associated to DAPs (Clerk et al., 1993). Alternative promoters and alternative splicing give rise to the utrophin protein family: full-size utrophin (400 kDa), DRP-1 (116 kDa) and Up71 (70 kDa), which have different tissue localizations (Wilson et al., 1999). Utrophin has an N-terminal actin-binding domain, which links the actin cytoskeleton to the plasma membrane. From the functional point of view, the C-terminus of both protein families comprises several domains for DAP binding (Winder, 1997).

On the cytoplasmic side of the DAPC, dystrophin binds to dystrobrevins providing a scaffold for binding to syntrophins ( $\alpha$ ,  $\beta$ 1,  $\beta$ 2,  $\gamma$ 1,  $\gamma$ 2), modular proteins that link ion channels, aquaporin channels and signaling proteins to the C-terminus of dystrophins, utrophins and dystrobrevins (Yang et al., 1995). Dp71 and DAPs are also expressed in non-muscular tissues including the central nervous system (Daloz et al., 2001), kidney, liver (Loh et al., 2001) and spermatozoa (Hernández-González et al., 2001). Dp71 isoforms and DAPs are localized in specific domains of mammalian spermatozoa and, interestingly, they only express a product of the DMD gene (Hernández-González et al., 2001). Protein components of the DAPC show different localizations in mammalian spermatozoa,  $\alpha$ -syntrophin was located in the middle piece of both plasma membrane and flagellum, whereas  $\beta$ -dystroglycan was only located in the plasma membrane of the flagellar middle piece (Hernández-González et al., 2001).

Together, Dp71 and the F-actin cytoskeleton, through the  $\alpha$ -syntrophin PDZ domain, can anchor different ionic channels and signaling proteins to specific domains of the plasma membrane, named syntrophin-associated proteins (SAPs) (Fig. 1). Some proteins containing the PDZ ligand domain have been found in mammalian spermatozoa such as:  $K^+$  channels (Félix et al., 2002),  $Ca^{2+}$  channels (Darszon et al., 1999), aquaporin-7 and -8 (Calamita et al., 2001) and neural nitric oxide synthase (nNOS) (Hernández-González et al., 2001) (Fig. 1). These

molecules are involved in functional processes such as capacitation, acrosome reaction and motility. It was recently reported that the absence of Dp71 in mdx3cv and Dp71 null mice, disrupts the distribution of the Kir4.1 potassium channels in Müller glial cells without altering their expression (Connors and Kofuji, 2002; Dalloz et al., 2003). Therefore, the aim of the present investigation was to determine whether the absence of Dp71 also alters the distribution of nNOS and ion channels in dystrophic mdx3cv spermatozoa.

Fertility alterations in DMD patients have not been reported. However, a low reproductive rate has been observed in mdx3cv mice (Cox et al., 1993). To understand how the absence of Dp71 affects the DAPC in spermatozoa, we analyzed the localization and expression of  $\beta$ -dystroglycan and  $\alpha$ -syntrophin, in the dystrophic mutant mdx3cv and in wild-type mice. Our results indicate that these proteins were affected in mdx3cv mice. Furthermore, in the absence of Dp71, altered flagellar morphology increased, originating a new DMD phenotype. These abnormalities were partially corrected when the plasma membrane was removed with neutral detergents. Interestingly, Na<sup>+</sup> and K<sup>+</sup> channels and the presence and localization of nNOS were disrupted in mdx3cv spermatozoa. Moreover, a short utrophin product, Up71 was relocalized and upregulated in mdx3cv spermatozoa. These results indicate that Dp71 and its DAPC are essential components of the sperm functional protein scaffold, necessary for the anchorage of membrane proteins in specific sperm domains and for normal mammalian spermatozoa morphology.

## **Materials and Methods**

### **Chemicals**

All reagents were of analytical quality and purchased from Sigma (St Louis, MO). Nitrocellulose membranes, acrylamide and N,N'-methylene-bis-acrylamide and molecular weight markers were from Bio-Rad (Richmond, CA).

### **Antibodies**

JAF antibody was produced by D. Mornet and characterized by Rivier et al. (Rivier et al., 1999). Dys2 and DRP-1 antibodies against dystrophins and utrophins respectively, were purchased from Novocastra (Newcastle-upon-Tyne, UK) and nNOS type 1 from BD Transduction Laboratories (Lexington, NY).  $\beta$ -Actin and  $\beta$ -tubulin antibodies were from Sigma (St Louis, MO). Anti K<sup>+</sup> channel Kv1.1 antibody and its blocking peptide (sc-1118P) were purchased from Santa Cruz Biotechnology (Santa Cruz, CA). Anti-Na<sup>+</sup> channel antibody was produced and characterized by Trimmer et al. (Trimmer et al., 1989). Peroxidase HRP-labeled anti-rabbit IgG, HRP-labeled anti-mouse IgG, TRITC (tetramethyl rhodamine)-labeled anti-rabbit IgG and TRITC-labeled anti-mouse IgG were purchased from Jackson ImmunoResearch (West Grove, PA).

### **Animals**

C57BL/6 and heterozygote mdx3cv mutant mice strains were obtained from Jackson Lab. (Bar Harbor, ME), and were bred in our laboratory facilities. They

were identified by western blot analysis of brain extracts. All experiments complied with the international regulations for animal care and experimentation.

### **Spermatozoa isolation**

Cauda epididymal mouse sperm were collected from wild-type mice and mdx3cv retired male breeders by placing minced cauda epididymis in 1 ml modified Krebs-Ringer medium (Whitten's/HEPES-buffered). After 10 minutes, sperm in suspension were washed in 10 ml Krebs-Ringer medium by centrifugation at 600 g for 5 minutes. Sperm cells were pelleted and then resuspended to a final concentration of  $30 \times 10^6$  cells/ml and simultaneously processed for indirect immunofluorescence and western blotting. Aliquots for morphological analysis were fixed in 1.5% final concentration of formaldehyde (Hernández-González et al., 2001).

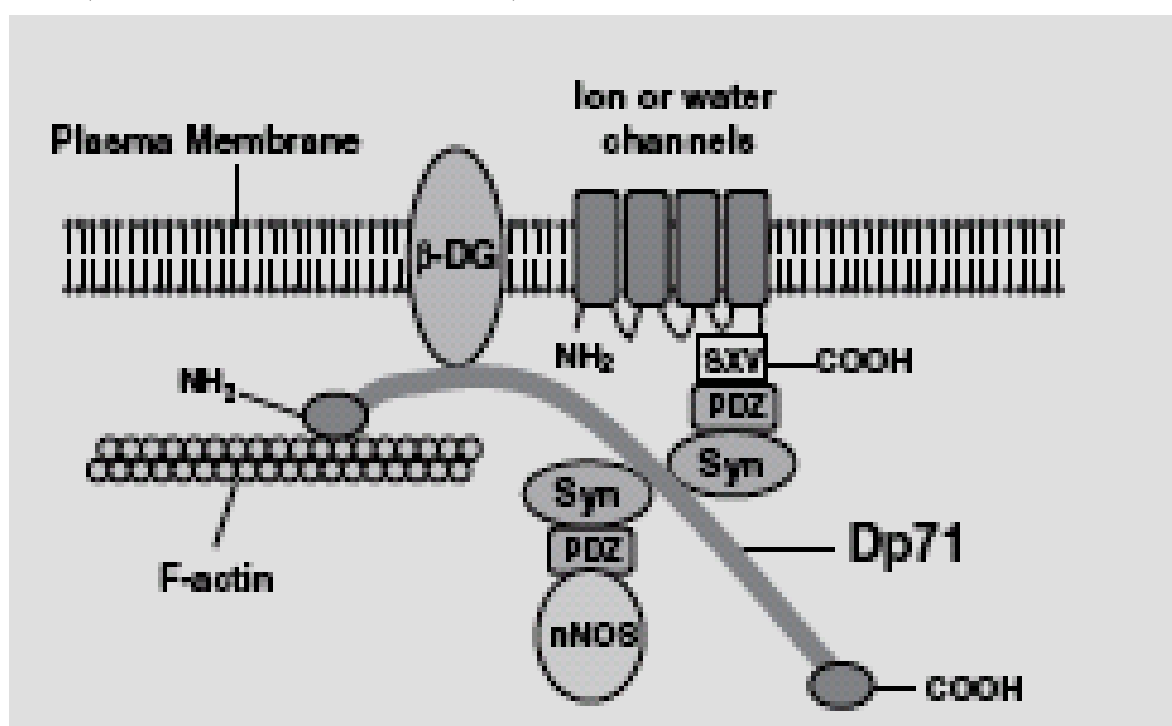


Fig. 1. Dp71-associated protein complex. The Dp71~DAPC is a multiprotein complex that connects the cytoskeleton to the plasma membrane of non-muscular cells. Dp71 has an actin-binding site at its N-terminal region (NH<sub>2</sub>). It forms a bridge between the actin cytoskeleton and the transmembrane protein β-dystroglycan (β-DG). β-dystroglycan interacts with Dp71, utrophin and actin via its cytoplasmic tail. Moreover, defects in β-dystroglycan are central to the pathogenesis of structural and functional neural abnormalities observed in DMD. On the cytoplasmic side of the complex, Dp71 binds to syntrophins (Syn) and dystrobrevins. Syntrophins are a family of five proteins (α, β1, β2, γ1 and γ2) containing two pleckstrin homology domains and a PDZ domain. The PDZ sequence serves as an adaptor for the recruitment of syntrophin-associated proteins (SAPs) such as: ion and water channels, receptors, kinases and neural nitric oxide synthase (nNOS). α-Syntrophin is the main isoform found in sperm. The localization of α- and β-dystrobrevins was unrelated to Dp71~DAPC localization in guinea pig spermatozoa (Hernández-González et al., 2001), thus we propose that they are components of flagellar structures. Like Dp71, Up71 is able to bind β-dystroglycan, syntrophins and F-actin. Therefore, it could compensate for Dp71 absence in mdx3cv spermatozoa, forming a Up71~DAPC with α-syntrophin.

### **Indirect immunofluorescence**

Sperm suspension samples were fixed in formaldehyde for 60 minutes at room temperature and centrifuged at 600 g for 4 minutes, washed, permeabilized and immunostained with appropriate antibodies, following a previously published protocol (Hernández-González et al., 2001). Spermatozoa were permeabilized in absolute acetone for 7 minutes at  $-20^{\circ}\text{C}$  and washed three times with PBS. Specific primary antibodies were added to the spermatozoa samples, incubated for 2 hours at  $37^{\circ}\text{C}$ , and then incubated with the respective TRITCconjugated secondary antibody. Samples were mounted in PBSglycerol (1:1) and examined with an epifluorescence microscope (Hernández-González et al., 2001). As negative controls sperm samples were treated with a non-specific first antibody; with only the secondary antibody; or with the anti-Kv1.1 antibody pre-incubated with the blocking peptide. All were then used for immunolocalization studies and western blotting. All controls gave negative results (data not shown).

### **Preparation of demembranated spermatozoa**

Wild-type and mdx3cv spermatozoa suspended in Krebs-Ringer medium were treated with the non-ionic detergent Brij-36T at 1.5% final concentration (Juárez-Mosqueda and Mújica, 1999), in the presence of protease inhibitors (4 mM PMSF, 4 mM pHMB, 2 mM pAB, 2 mM benzamidine, 1  $\mu\text{M}$  leupeptin, 1  $\mu\text{M}$  aprotinin and 1  $\mu\text{M}$  pepstatin) for 5 minutes at  $4^{\circ}\text{C}$ . This treatment solubilized sperm membranes and acrosomes. Immediately, the spermatozoa were centrifuged at 2000 g for 15 minutes at  $4^{\circ}\text{C}$  and the pellet (demembranated spermatozoa) was recovered. The spermatozoa were washed three times with buffer A (50 mM Tris-HCl, pH 7.4, 2 mM EGTA) and collected by centrifugation (2000 g for 15 minutes at  $4^{\circ}\text{C}$ ). The final pellet, containing demembranated spermatozoa, was fixed in formaldehyde, as above.

### **Isolation and solubilization of sperm membranes and flagella**

Spermatozoa from wild-type and mdx3cv mice were resuspended in buffer A with the protease inhibitor mixture and sonicated for 15 seconds at 40 watts (Ultrasonic Processor, Daigger Co., Vernon Hills, IL). This process breaks sperm membranes (plasma and acrosomal) and separates the heads from the flagella. Flagella were then collected by centrifugation at 1000 g for 30 minutes, at  $4^{\circ}\text{C}$ . The supernatant was saved for membrane isolation and the pellet was resuspended in buffer A and layered onto a two-step Percoll gradient (70/95%) and centrifuged for 20 minutes at 600 g at  $4^{\circ}\text{C}$ . The bottom pellet, containing heads without acrosome was discarded and the flagellar fraction was collected from the Percoll interface. Then, the flagellar fractions were resuspended in buffer A plus protease inhibitor mixture, and solubilized by DTT-SDS treatment (Júarez-Mosqueda and Mújica, 1999). Sperm membranes (plasma and acrosomal membranes) were recovered from the 1000 g supernatant and centrifuged at 100,000 g for 60 minutes at  $4^{\circ}\text{C}$ . The pellet was solubilized in SDS (Hernández-González et al., 2000). Proteins from the solubilized sperm fractions were separated by electrophoresis and processed for western blotting.

### **Protein extracts**

Spermatozoa (50×10<sup>6</sup> cell/ml), isolated sperm membranes and isolated flagella, resuspended in 50 mM Tris-HCl and 2 mM EDTA, pH 7.4, containing the protease inhibitor mixture, were treated with 1% SDS (final concentration) and were then boiled for 5 minutes and centrifuged at 10,000 g for 5 minutes. The supernatants were used for total protein determination and processed for electrophoresis and western blotting.

### **Electrophoresis and western blotting**

Sperm membranes and flagellar fractions were analyzed by SDS-PAGE (using 10% or 6% acrylamide) and transferred to nitrocellulose membranes. For detection of specific proteins, the nitrocellulose membranes were incubated for 2 hours at 37°C with specific antibodies and then with an appropriate secondary antibody coupled to HRP, developed by an ECL chemiluminescence kit (Amersham) and recorded on film (X-Omat, Kodak) (Hernández-González et al., 2001).

### **Morphological studies**

Whole and Brij-treated spermatozoa from wild-type and mdx3cv mice were fixed in formaldehyde (1.5% final concentration). Sperm morphology was examined by phase-contrast microscopy and classified as follows: (1) with normal flagella, not curved or twisted; (2) with curved flagella in the middle piece; and (3) with twisted flagella. To evaluate flagellar alterations, 1000 spermatozoa (n=5) from each mouse strain were classified and counted. The data were analyzed by Student's t-test using the Sigma-Stat software.

## **Results**

### **Mdx3cv spermatozoa show increased frequency of abnormal flagellar morphology**

To determine possible morphologic alterations of spermatozoa from dystrophic mice, we compared mdx3cv and wild-type spermatozoa cell shape. Major changes were only found in the flagellum, three types of flagella were observed: normal (Fig. 2A1), and two altered morphologies: one with curved (or bent) flagella at the middle piece level (Fig. 2A2) and another with twisted flagella (Fig. 2A3). These flagellar morphologies were found in different proportions in sperm samples from wild-type or mdx3cv mice. Evaluation by optical microscopy (1000 sperm cells, n=5) of wild-type spermatozoa showed that 84% presented normal flagellar morphology and only 16% had anomalous flagellar: 10% were sperm with bent flagella and 6% had twisted flagella (Fig. 2B, black bars). In contrast, 46% of mdx3cv spermatozoa showed normal morphology, 46% presented curved flagella and 8% exhibited a twisted form (Fig. 2B, white bars). When spermatozoa were treated with Brij- 36T, a neutral

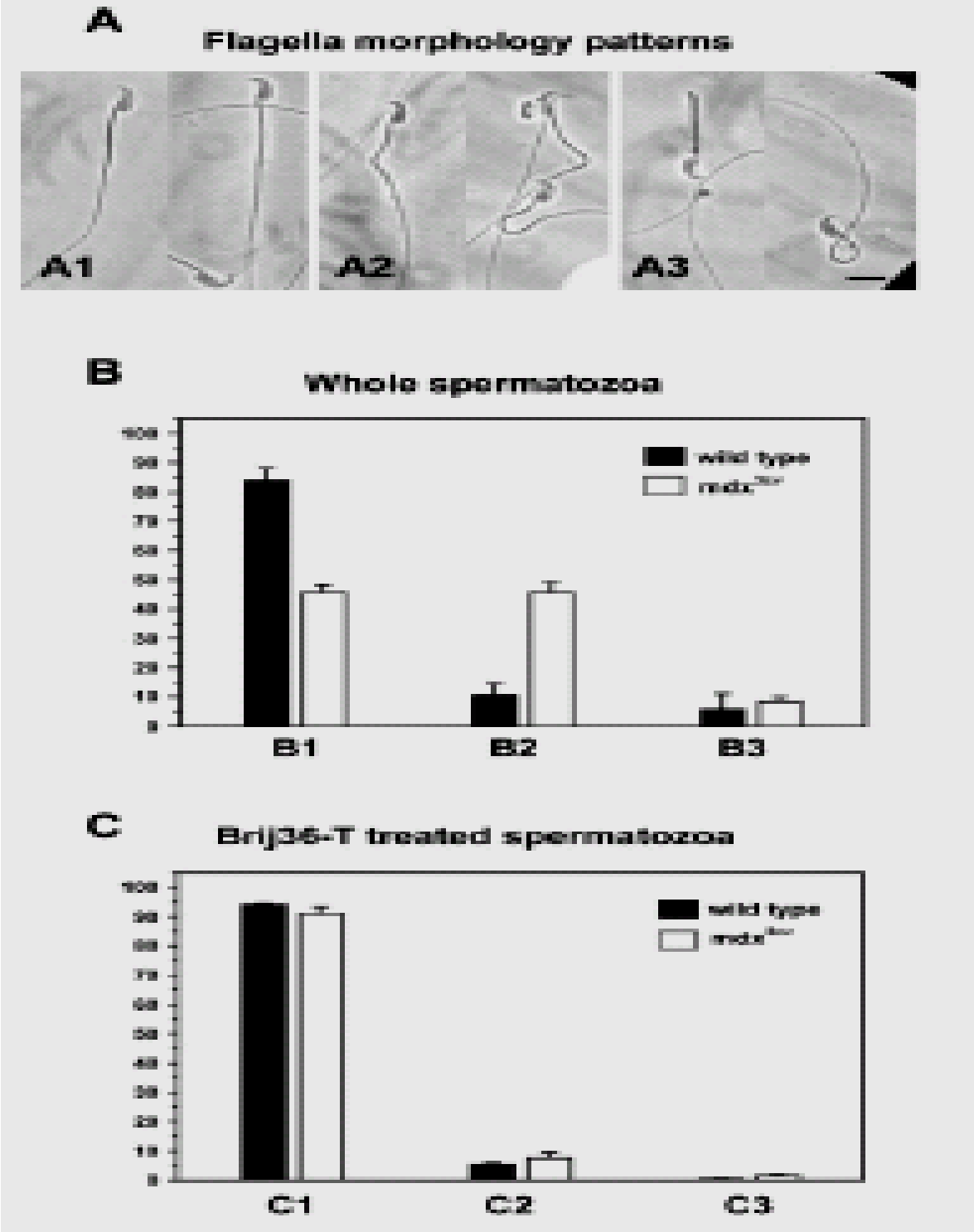


Fig. 2. Altered morphology in mdx3cv mouse spermatozoa. (A) Flagellar morphology patterns from wild-type and mdx3cv mice were analyzed and quantified by phase-contrast microscopy. Different sperm samples of both strains presented the classic normal morphology (A1), as well as two different abnormalities: curved (A2) and twisted flagella (A3). (B) Quantification of flagellar morphology patterns, normal shape (B1), curved (B2) and twisted flagella (B3). (C) Quantification of flagellar morphology patterns of Brij-36T treated spermatozoa: normal flagella (C1), curved flagella (C2) and twisted flagella (C3). Black bars for wild-type mice and white bars for mdx3cv mice. The data in these graphs represent the mean $\pm$ s.e. from five independent experiments. Bar, 6  $\mu$ m.



detergent that solubilizes the sperm membranes and acrosome (Juárez-Mozqueda and Mújica, 1999), most sperm cells from mdx3cv recovered their normal morphology (91%) and only 8% showed curved flagella (Fig. 2C). The ratio of normal to abnormal flagella from demembranated spermatozoa is similar in both strains (Fig. 2C). These morphological alterations are a new phenotype and the Dp71~DAPC could be related to these alterations, it was therefore investigated in wild-type and mdx3cv spermatozoa.

### **Presence of Dp71 in wild-type and mdx3cv mice spermatozoa**

To examine the level and localization of Dp71 in wild-type and mdx3cv mice spermatozoa, indirect immunofluorescence and western blotting analyses were performed. In spermatozoa from wild-type mice, immunoreactivity of Dys-2 antibody was concentrated as granular staining in the middle piece and in the postacrosomal region (Fig. 3A1). Staining was undetectable in spermatozoa from mdx3cv mice (Fig. 3A2), confirming the genotype of this dystrophic animal model. Again, we observed the remarkable difference between the morphology of spermatozoa from dystrophic animals and from wild-type mice in the phase contrast images (see Fig. 2A). We characterized the presence of dystrophins by western blotting of the sperm membrane fraction extracts from wild type and mdx3cv mice. Only one protein band with apparent molecular mass 76 kDa was clearly identified in wild-type sperm cell membranes, which corresponded to Dp71 and was undetectable in mdx3cv spermatozoa membrane fractions (Fig. 3B). No other Dps were detected in spermatozoa protein extracts. As expected, the mdx3cv mutation abolished the presence of Dp71 as demonstrated here.

### **The distribution of Up71 changes in mdx3cv spermatozoa**

In order to determine if some DRP can compensate for the decreased expression or absence of Dp71 in mdx3cv, we analyzed the concentration and distribution of utrophins in wild-type and mdx3cv spermatozoa. Fig. 4 compares the localization and presence of utrophins in whole spermatozoa. DRP-1, anti-utrophin antibody, exclusively stained the postacrosomal region of whole spermatozoa from wild-type mice (Fig. 4A1). Analysis of mdx3cv spermatozoa revealed fluorescence in the middle piece and more intense staining in the whole head (Fig. 4A2). Fluorescence was also more evident in dystrophic compared to control spermatozoa. In addition, utrophin concentration was analyzed by western blotting using purified membranes from wild-type and mdx3cv mice and as a control for protein concentration,  $\beta$ -actin was detected simultaneously. Fig. 4B shows that the DRP-1 antibody revealed only one protein band of 76 kDa corresponding to Up71. The level of Up71 was higher in membrane fractions of mdx3cv spermatozoa compared to wild-type spermatozoa, confirming the more concentrated Up71 fluorescence observed by indirect immunofluorescence. No other utrophin proteins were detected in spermatozoa extracts. Therefore, in the absence of Dp71, Up71 was upregulated and redistributed, from the postacrosomal region to the middle piece and the head of spermatozoa.



Fig. 3. Genotype confirmation of mdx3cv spermatozoa. (A) Expression and localization of Dp71 in spermatozoa from control and mdx3cv mice were determined by indirect immunofluorescence and western blotting using Dys2 antibody. Immunostaining in wild-type spermatozoa was localized in the postacrosomal region and in the middle piece of the flagella (A1). The absence of Dys2 immunostaining in mdx3cv spermatozoa confirms their genotype (A2). A1' and A2' show phase-contrast images corresponding to spermatozoa from wild-type and mdx3cv mice. (B) The presence of dystrophin products was analyzed by western blotting. In membrane fractions from wild-type spermatozoa only one protein band of 76 kDa was detected, corresponding to Dp71 (B1). In the membrane fraction of mdx3cv spermatozoa, Dp71 was absent and no other dystrophin was found (B2).

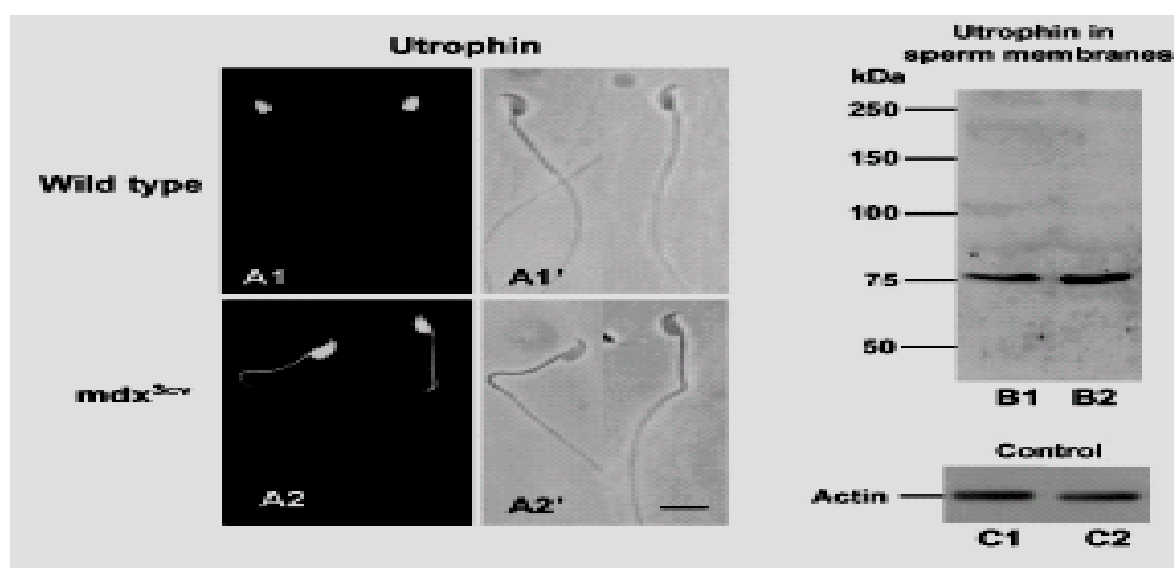
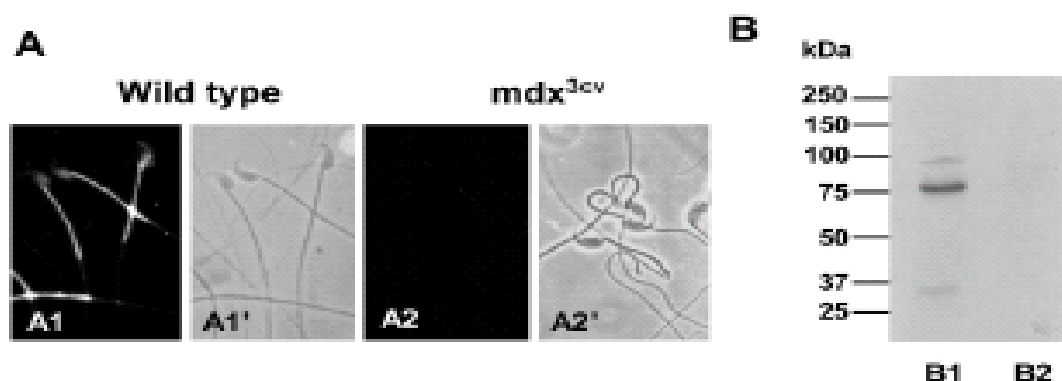


Fig. 4. The localization and concentration of utrophin in mdx3cv spermatozoa. (A) Spermatozoa from wild-type and mdx3cv strains were analyzed by indirect immunofluorescence and western blotting using DRP-1 anti-utrophin antibody. Utrophin immunostaining was exclusively observed in the postacrosomal region of wild-type whole spermatozoa (A1). In mdx3cv spermatozoa, DRP-1 staining was localized in the whole head and flagellar middle piece (A2). (B) In protein extracts of sperm-isolated membranes from wild-type and mdx3cv spermatozoa, only one protein band corresponding to Up71 was detected in both membrane protein extracts. Up71 was more concentrated in membranes from mdx3cv spermatozoa (B2) than in membranes from wild-type spermatozoa (B1). A similar concentration of  $\beta$ -actin was detected in membrane fractions from wild-type (C1) and mdx3cv mice (C2). Bar, 6  $\mu$ m.

### **The localization of DAPC is altered in the absence of Dp71**

We previously demonstrated that non-muscle cells express some members of the DAPC that were altered by the absence of Dp71 (Daloz et al., 2001). To examine possible perturbations of the DAPC owing to the absence of Dp71 in mdx3cv mice, we used specific antibodies against  $\beta$ -dystroglycan and  $\alpha$ -syntrophin to analyze their respective localization and presence in spermatozoa.  $\beta$ -dystroglycan distribution was compared by indirect immunofluorescence, using the JAF polyclonal antibody and it was localized in the postacrosomal region and the flagellar middle piece of wild-type spermatozoa (Fig. 5A1). In contrast,  $\beta$ -dystroglycan immunostaining was observed as very faint fluorescence in the mdx3cv spermatozoa (Fig. 5A2) and in some cells it was not detectable at all (data not shown), indicating low or no presence in the flagellar middle piece. Protein levels in mdx3cv and wild-type spermatozoa were analyzed by western blotting. Only one protein was detected in the wild-type sperm membrane fraction as a band with of ~50 kDa (Fig. 5D1), however, it decreased (Fig. 5D2) or was absent (data not shown) in membranes from mdx3cv spermatozoa. As previously reported for guinea pig spermatozoa,  $\beta$ -dystroglycan is only present in sperm plasma membrane, therefore, it was not detected in spermatozoa without membranes from wild-type and mdx3cv mice (data not shown).

In addition, the distribution of  $\alpha$ -syntrophin was analyzed. Indirect immunofluorescence with C4 polyclonal antibody clearly revealed  $\alpha$ -syntrophin staining concentrated in the middle piece of the flagellum and the postacrosomal region of whole sperm cells from the wild-type strain (Fig. 5B1), whereas in demembranated cells it was only localized in the flagellar middle piece (Fig. 5C1) as was observed for guinea pig spermatozoa (Hernández-González et al., 2001). The  $\alpha$ -syntrophin immunoreactivity in whole spermatozoa from dystrophic animals was concentrated in the middle piece and the whole head (Fig. 5B2). In demembranated mdx3cv spermatozoa  $\alpha$ -syntrophin staining was relocated in the postacrosomal region and along the flagella (Fig. 5C2). It was evident that  $\alpha$ -syntrophin was clearly redistributed in mdx3cv spermatozoa with normal or abnormal flagella (Fig. 5B2'). In addition,  $\alpha$ -syntrophin staining was increased in the mutant strain (Fig. 5B2,C2), compared to the wild-type strain (Fig. 5B1,C1). To test whether in spermatozoa of the dystrophic strain,  $\alpha$ -syntrophin was more concentrated than in the wild-type strain, they were analyzed by western blotting. Fig. 5 also shows the comparative level of  $\alpha$ -syntrophin (55 kDa) in sperm membranes (E1,E2) and purified flagella (F1,F2) from wild-type and mutant mice, respectively. It is evident that the  $\alpha$ -syntrophin level was increased in both mdx3cv sperm fractions: membranes and flagella (Fig. 5E2,F2, respectively), compared with the same subcellular fractions from wild-type spermatozoa (Fig. 5E1,F1, respectively).

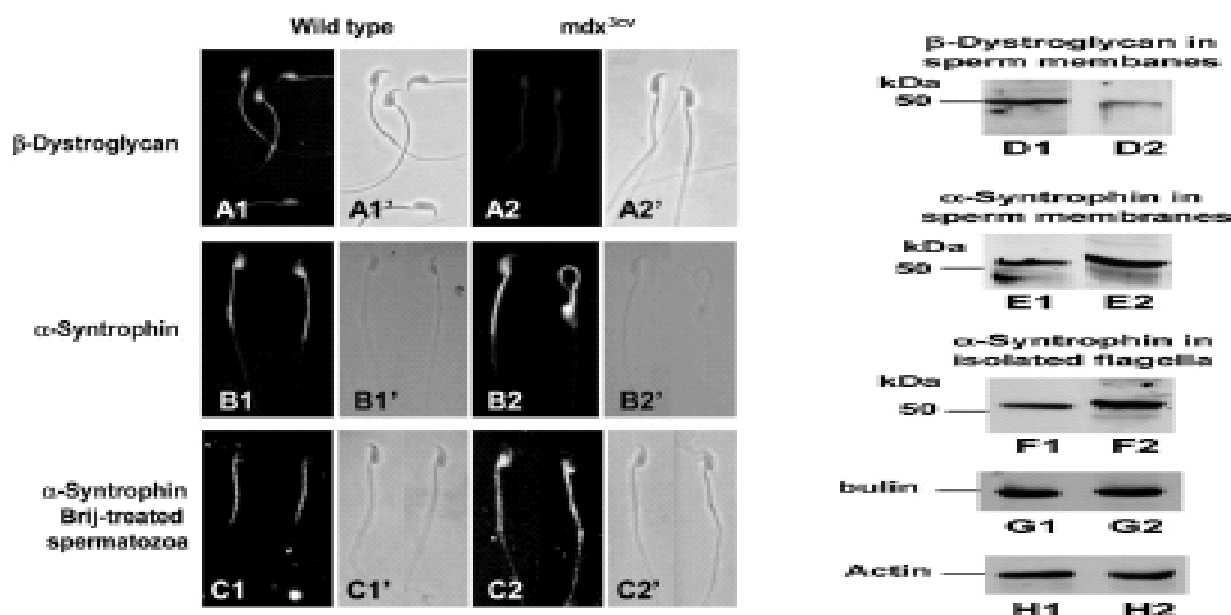


Fig. 5. Localization and presence of DAPs:  $\beta$ -dystroglycan and  $\alpha$ -syntrophin in mdx3cv spermatozoa.  $\beta$ -Dystroglycan and  $\alpha$ -syntrophin were detected by indirect immunofluorescence and western blotting using specific antibodies. (A) Images show the localization of  $\beta$ -dystroglycan in the postacrosomal region and in the flagellar middle piece of wild-type spermatozoa (A1). The fluorescence was very weak or absent (data not shown) in spermatozoa from the mdx3cv strain (A2). (B)  $\alpha$ -Syntrophin staining was found in the postacrosomal region and the middle piece of wild-type whole spermatozoa (B1). In contrast, in mdx3cv spermatozoa,  $\alpha$ -syntrophin immunofluorescence appeared brightly stained in the whole head and in the middle piece of the flagellum and weak staining was detected in the first portion of the flagellar principal piece (B2). (C) In demembranated wild-type spermatozoa,  $\alpha$ -syntrophin was only localized in the middle piece (C1), whereas in demembranated mdx3cv spermatozoa it was redistributed along the flagella and in the postacrosomal region (C2). Western blotting analysis of

sperm extracts was performed for each protein. (D) JAF antibody revealed that the  $\beta$ -dystroglycan (50 kDa) was more concentrated in membranes from wildtype (D1) than in mdx3cv (D2) spermatozoa. (E,F) Levels of  $\alpha$ -syntrophin (55 kDa) were comparable in membrane fractions (E1,E2) and in isolated flagellar fractions (F1,F2).  $\alpha$ -Syntrophin was more concentrated in membranes (E2) and flagellar (F2) fractions from mdx3cv spermatozoa, than in membranes (E1) and flagellar (F1) fractions from wild-type spermatozoa.  $\beta$ -Tubulin (G) and  $\beta$ -actin (H) were detected in flagellar and membrane fractions and their levels were used as loading controls.

The results described above prove that the Dp71 mutation affects the DAPC level in the flagellar middle piece and show that  $\alpha$ -syntrophin is abundant and redistributed along the flagellum and the head. These results indicate that the absence of Dp71 affects the DAPC components in opposite ways: decreasing the concentration of  $\beta$ -dystroglycan and increasing the concentration of  $\alpha$ -syntrophin.  $\text{Na}^+$  and  $\text{K}^+$  channels and nNOS are redistributed in mdx3cv mice According to previous work Dp71, DAPs ( $\beta$ -dystroglycan and  $\alpha$ -syntrophin), nNOS (Hernández-González et al., 2001),  $\text{K}^+$  channels (Félix et al., 2002) and AQP-7 (Calamita et al., 2001) are distributed within similar compartments of the spermatozoa plasma membrane. Moreover, in brain and muscle,  $\alpha$ - syntrophin is thought to recruit several SAPs (Gee et al., 1998).

It is known that the PDZ domain of syntrophins is involved in the interaction with these proteins (Brenman et al., 1996). As we found that  $\alpha$ -syntrophin is clearly redistributed and more concentrated in mdx3cv spermatozoa, we were interested in the effect of this alteration, or the absence of other DAPC components, on the presence and localization of different membrane ion channels and signaling proteins such as nNOS.

First, we investigated whether the absence of Dp71 modifies the distribution of voltage-dependent  $\text{Na}^+$  ( $\mu 1$ ) and  $\text{K}^+$  (Kv1.1) channels and nNOS, three important SAPs involved in specific spermatozoa functions. Immunostaining of  $\text{Na}^+$  channels was observed in the postacrosomal region and the flagellar middle piece, and weak staining was present in the flagellar principal piece of wild-type spermatozoa (Fig. 6A1). However, in mdx3cv spermatozoa, immunoreactivity to  $\text{Na}^+$  channels was concentrated in the whole head with less staining found in the middle piece (Fig. 6A2). The immunolocalization for  $\text{K}^+$  channels (anti-Kv1.1 antibody) in wild-type spermatozoa showed that it was concentrated in the whole head and slightly in the middle piece (Fig. 6B1). In mdx3cv spermatozoa,  $\text{K}^+$  channel localization was completely altered, it was present in whole spermatozoa and specially concentrated in the acrosome region and in the middle piece (Fig. 6B2). It is remarkable that the redistribution of the Kv1.1 channels in spermatozoa of the mdx3cv strain (Fig. 6B2) was similar to that observed for  $\alpha$ -syntrophin redistribution (Fig. 5B2,C2). As  $\text{Na}^+$  and  $\text{K}^+$  channels are membrane proteins, they were not detected in demembranated spermatozoa (data not shown).

In the wild-type strain, nNOS immunostaining was detected in the flagellar middle piece and in the postacrosomal region (Fig. 6C1), as was Dp71 (see Fig. 3A1). In mdx3cv spermatozoa, nNOS was more concentrated in the whole head and also in the middle piece (Fig. 6C2). In membrane-free spermatozoa of both strains, nNOS was immunolocalized in the middle piece, where mitochondria are condensed (data not shown). A clear redistribution and a considerable increase in staining were observed for these three proteins in mdx3cv spermatozoa.

We analyzed the presence of K<sup>+</sup> and Na<sup>+</sup> channels and nNOS in membrane fractions of wild-type and mdx3cv spermatozoa by western blotting and, as control of protein concentration,  $\beta$ -actin was detected simultaneously. Fig. 6 shows the detection of Na<sup>+</sup> and K<sup>+</sup> channels and nNOS in isolated membrane fractions from wild-type and mdx3cv spermatozoa. It was evident that protein bands were expressed in membrane fractions, identified by their molecular weight: 210 kDa for the Na<sup>+</sup> channels (Fig. 6D1,D2), 60 kDa for the K<sup>+</sup> channels (E1,E2), 130 kDa for nNOS (F1,F2) and 45 kDa for  $\beta$ -actin (G1,G2). In membranes of mdx3cv spermatozoa, Na<sup>+</sup> channels and nNOS were clearly present in high concentrations, and K<sup>+</sup> channels were increased to a lesser proportion. These results confirmed that the increased staining observed by immunofluorescence for Na<sup>+</sup>, K<sup>+</sup> channels and nNOS was real. In addition, we provide the first detection and localization of a Na<sup>+</sup> channel in mammalian spermatozoa.

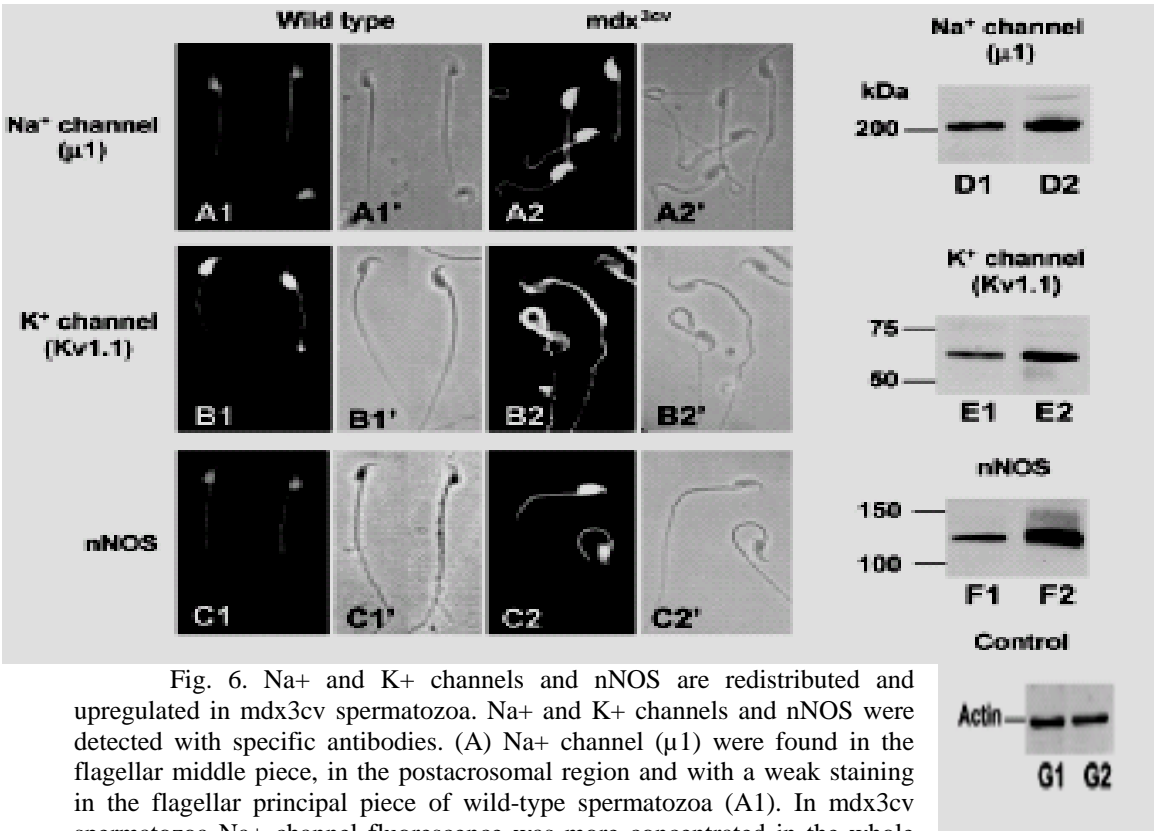


Fig. 6. Na<sup>+</sup> and K<sup>+</sup> channels and nNOS are redistributed and upregulated in mdx3cv spermatozoa. Na<sup>+</sup> and K<sup>+</sup> channels and nNOS were detected with specific antibodies. (A) Na<sup>+</sup> channel ( $\mu$ 1) were found in the flagellar middle piece, in the postacrosomal region and with a weak staining in the flagellar principal piece of wild-type spermatozoa (A1). In mdx3cv spermatozoa Na<sup>+</sup> channel fluorescence was more concentrated in the whole head and a discrete staining was detected in the middle piece (A2).

(B) In contrast, K<sup>+</sup> channels (Kv1.1) were concentrated in the whole head and weak staining was detected in the middle piece of wild-type spermatozoa (B1). The fluorescence pattern of K<sup>+</sup> channels for mdx3cv spermatozoa was localized in the head and along the flagellum (B2). (C) nNOS was localized at the postacrosomal region and middle piece of wild-type spermatozoa (C1) and it was more concentrated in the whole head and middle piece of mdx3cv spermatozoa (C2). (D,E,F) Western blotting of Na<sup>+</sup>, K<sup>+</sup> channels and nNOS in membrane fractions obtained from wild-type or mdx3cv spermatozoa was performed. The proteins detected were identified by their molecular weight: 210 kDa for Na<sup>+</sup> channels, 60 kDa for K<sup>+</sup> channels and 130 kDa for nNOS, in wild-type (D1, E1 and F1, respectively) and mdx3cv spermatozoa (D2,E2,F2, respectively).  $\beta$ -Actin was detected in the same membrane fractions as a control for the wild type (G1) and for mdx3cv (G2).

## Discussion

Previous reports have shown that the absence of dystrophin gene products results in a loss of members of the DAPC from cell membrane in muscle, brain and retina (Blake et al., 2001). Our study aimed to compare the distribution of DAPC components in mdx3cv spermatozoa, which lack the expression of all DMD gene products. We have shown that mouse spermatozoa exclusively contain dystrophin Dp71. To elucidate the role(s) of Dp71, we studied mdx3cv spermatozoa and found that its absence resulted in: (1) an increase in abnormal flagellar morphology; (2) an increased level and redistribution of Up71,  $\alpha$ -syntrophin, Na<sup>+</sup> and K<sup>+</sup> channels ( $\mu$ 1 and Kv1.1, respectively) and nNOS; and (3) a dramatic reduction in the level of  $\beta$ -dystroglycan.

The actin scaffold associated with the plasma membrane is important for sperm morphogenesis and differentiation (Ozaki- Kuroda et al., 2002), and its alteration produces defective sperm morphogenesis and male-specific infertility (Bouchard et al., 2000). Dp71 and  $\beta$ -dystroglycan are minor actin-binding proteins required for anchorage of the cytoskeleton to the plasma membrane through the DAPC (Howard et al., 1998; Chen et al., 2003). We showed that mdx3cv mice produced an increased number of sperm with aberrant flagellar morphology, which could be a consequence of Dp71 absence and reduction of levels of  $\beta$ -dystroglycan. These alterations could modify the anchorage of the cytoskeleton to the plasma membrane. In agreement with this proposal is the rectification of the abnormal shape observed when the plasma membrane of mdx3cv spermatozoa was removed, indicating the importance of the cytoskeletal interaction with the plasma membrane for flagellar morphology. Our results also show that the sperm alterations significantly reduced (almost 50%) the number of spermatozoa capable of fertilization. These abnormal spermatozoa had deficient motility, consisting of vibratory movements of the flagella without displacement (data not shown). This is the first description of a phenotype that results in a morphologic alteration of a non-muscular cell in dystrophic mice.

The most diminished or sometimes absent DAP in the mdx3cv spermatozoa was  $\beta$ -dystroglycan, which agrees with a recent observation in retina, where it was severely reduced in Dp71 null mice (Dalloz et al., 2003). Conversely, the absence of Dp71 in mdx3cv spermatozoa resulted in  $\alpha$ -syntrophin relocalization and upregulation. It should be noted that the absence of Dp71 in mdx3cv spermatozoa perturbs two members of the DAPC,  $\beta$ -dystroglycan and  $\alpha$ -syntrophin, in different ways. In both cases, our results suggest that Dp71 is important for the formation and/or stabilization of the DAPC. Members of the utrophin and dystrophin families are structurally homologous and it seems very likely that they perform similar functions. In mdx3cv mice, the increased level of utrophin ameliorates the pathology of dystrophin deficiency (Tinsley et al., 1996). Up71, a member of the utrophin family, is relatively abundant in several non-muscular tissues including the testis (Wilson et al., 1999) and is able to bind DAPs such as  $\beta$ -dystroglycan, syntrophins and dystrobrevins (Blake et al., 2001). In mdx3cv spermatozoa Up71 is upregulated and redistributed and may compensate for the absence of Dp71,



forming a Up71~DAPC with  $\alpha$ -syntrophin, and in this way, Na<sup>+</sup> and K<sup>+</sup> channels and nNOS could be anchored to the plasma membrane from the head and middle piece. The similar Up71 and  $\alpha$ -syntrophin relocalization in mdx3cv spermatozoa allows us to speculate about dystrophin-like complexes organized to compensate for Dp71 absence (Fig. 7). Therefore, the K<sup>+</sup> channel localized in the plasma membrane of the principal piece could only be anchored by  $\alpha$ -syntrophin, because Up71 is absent in this sperm region (Fig. 7). These results suggest that in each plasma membrane compartment of mdx3cv spermatozoa the Up71~DAPC may be different, as described for the dystrobrevin complex in different regions of the kidney (Loh et al., 2001). Moreover, this complex may partially compensate for Dp71 absence in mdx3cv spermatozoa with normal flagella and may be responsible for dystrophic mouse reproduction. However, Up71~DAPC may also establish a different relationship with the sperm cytoskeleton, producing incorrect flagellar development. To prove this proposition, it is necessary to compare the in vitro fertilization capacity of both kinds of sperm cells, or of spermatozoa from mdx3cv/utr<sup>-/-</sup> mice. Ion and water channels have a subcellular localization and tissue-specific expression patterns that determine their physiological roles, although, in spermatozoa, their localization and the mechanism of anchoring remain unknown (Darszon et al., 1999). In this study we found that Dp71~DAPC may participate in the scaffold that contributes to anchor some membrane SAPs such as K<sup>+</sup> and Na<sup>+</sup> channels and nNOS in wild-type spermatozoa (see Fig. 7). Interestingly, all of them were upregulated in spermatozoa from mdx3cv mice.

These observations are different from those reported in retinal glial Müller cells of Dp71 null mice, where the K<sup>+</sup> channel Kir 4.1 remained unchanged and aquaporin-4 was downregulated (Daloz et al., 2003). The upregulation and redistribution of Na<sup>+</sup> and K<sup>+</sup> channels and nNOS may depend on a compensatory process for the Dp71~DAPC alteration, which apparently does not correct the sperm morphologic phenotype. The presence of voltage-dependent Na<sup>+</sup> channels in mammalian spermatozoa has been suggested by the detection of sodium currents, which were inhibited by specific blockers (Shi and Ma, 1998; Patrat et al., 2000). The above evidence supports our result for the presence of a voltage-dependent Na<sup>+</sup> channel ( $\mu$ 1), which was codistributed with Dp71~DAPC in mouse sperm. To the best of our knowledge, it is the first time that a voltage-dependent Na<sup>+</sup> channel was detected and localized by immunological procedures in mammalian sperm (Patrat et al., 2000). Its role in capacitation, acrosome reaction and/or motility remains to be determined.

The specific localization of ion channels suggests that they could produce ionic environments in specific sperm domains, which may be affected by their increased presence and redistribution, as shown here for spermatozoa from dystrophic mice. These altered ion environments may modify some sperm processes in mdx3cv spermatozoa and consequently decrease their fertility. Hence, the adequate presence and localization of ion channels and the anchorage of the actin cytoskeleton seem very important for sperm physiology.



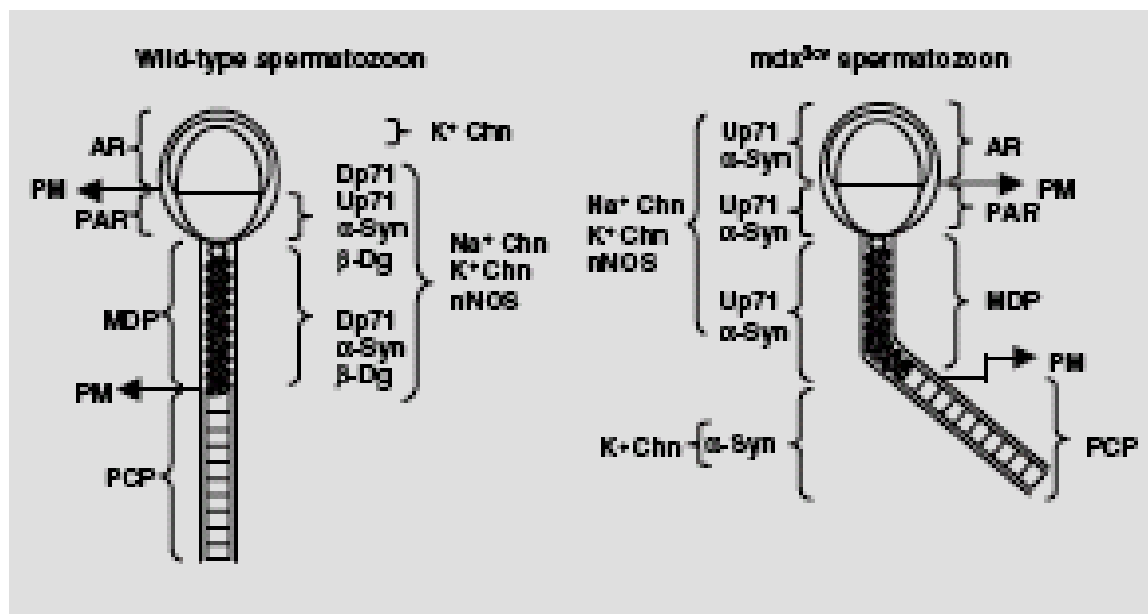


Fig. 7. Schematic representation of wild-type and mdx3cv spermatozoa showing the localization of Dp71~DAPC or Up71~DAPC. Dp71 or Up71 complex and SAPs (ion channels and nNOS) are based on indirect immunofluorescence localization and western blotting detection in whole spermatozoa, demembranated spermatozoa and plasma membrane data. a-Syn, a-syntrophin; AR, acrosome region; β-Dg, β-dystroglycan; Dp71, short dystrophin non-spliced for exon 78; K+Chn, K+ channel (Kv1.1); MDP, middle piece; Na+Chn, Na+ channel (μ1); nNOS, neural nitric oxide synthase; PAR, postacrosomal region; PCP, principal piece; PM, plasma membrane; Up71, short utrophin.

### Acknowledgement:

We are grateful to Gérald Hugon for antibody production, to Juan Carlos Garcia for mdx3cv mouse care, to Aurora Candelaria for mice genotyping and to Ana Lilia Roa Espitia for her assistance in sperm preparation. Isabel Pérez Montfort corrected the English version of the manuscript. This work was partially supported by the CONACYT grant No. 34819 to E.O.H.-G. and The Association Francaise Contre les Myopathies to D.M. and A.R.

### References

- Austin, R. C., Morris, G. E., Howard, P. L., Klamut, H. J. and Ray, P. N. (2000). Expression and synthesis of alternatively spliced variants of Dp71 in adult human brain. *Neuromuscul. Disord.* 10, 187-193.
- Blake, D. J., Weir, A., Newey, S. E. and Daives, K. E. (2001). Function and genetics dystrophin and dystrophin-related proteins in muscle. *Physiol. Rev.* 82, 291-329.

Bouchard, M. J., Dong, Y., McDermonett, B. M., Lam, D.-H., Jr, Brown, K. R., Shelanski, M., Bellvé, A. B. and Rancaniello, V. R. (2000). Defects in nuclear and cytoskeleton morphology and mitochondrial localization in spermatozoa of mice lacking Nectin-2, a component of cell-cell adherents junctions. *Mol. Cell. Biol.* 20, 2865-2873.

Brenman, J. E., Chao, D. S., Gee, S. H., McGee, A. W., Craven, S. E., Santillano, D. R., Wu, Z., Huang, F., Xia, H., Peters, M. F., Froehner, S. C. and Bredt, D. S. (1996). Interaction of nitric oxide synthase with the postsynaptic density protein PDS-95 and alpha 1-syntrophin mediated by PDZ. *Cell* 84, 757-767.

Calamita, G., Mazzone, A., Cho, Y. S., Valenti, G. and Suelto, M. (2001). Expression and localization of the aquaporin-8 water channel in rat testis. *Biol. Reprod.* 64, 1660-1666.

Chávez, O., Harricane, M. C., Alemán, V., Dorbani, L., Larroque, C., Mornet, D., Rendón, A. and Martínez-Rojas, D. (2000). Mitochondrial expression of a short dystrophin-like product with molecular weight of 71 kDa. *Biochem. Biophys. Res. Comm.* 274, 275-280.

Chen, Y. J., Spence, H. J., Cameron, J. M., Jess, T., Isley, J. L. and Winder, S. J. (2003). Direct interaction of  $\beta$ -dystroglycan with F-actin. *Biochem. J.* 375, 329-337.

Clerk, A., Morris, G. E., Dubowitz, V., Davies, K. E. and Sewry, C. A. (1993). Dystrophin-related protein, utrophin, in normal and dystrophic human fetal skeletal muscle. *Histochem. J.* 25, 554-561.

Connors, N. C. and Kofuji, P. (2002). Dystrophin Dp71 is critical for the clustered localization of potassium channels in retinal glial cells. *J. Neurosci.* 22, 4321-4327.

Cox, A. G., Phelps, F. S., Chapman, V. M. and Chamberlain, J. S. (1993). New mdx mutation disrupts expression of muscle and non-muscle isoforms of dystrophin. *Nat. Genet.* 4, 87-93.

Dalloz, C., Claudepierre, T., Rodius, F., Mornet, D., Sahel, J. and Rendón, A. (2001). Differential distribution of the members of the dystrophin glycoprotein complex in mouse retina: effect of the mdx3cv mutation. *Mol. Cell. Neurosci.* 17, 908-920.

Dalloz, C., Sarig, R., Fort, P., Yaffe, D., Bordais, A., Pannicke, T., Grosche, J., Mornet, D., Reichenbach, A., Sahel, J., Nudel, U. and Rendón, A. (2003). Targeted inactivation of dystrophin gene product Dp71: phenotypic impact in mouse retina. *Hum. Mol. Genet.* 12, 1543-1554.

Darszon, A., Labarca, P., Nishigaki, T. and Espinosa, F. (1999). Ion channels in sperm physiology. *Physiol. Rev.* 79, 481-509.

Ervasti, J. M. and Campbell, K. P. (1993). A Role for the dystrophin glycoprotein complex as a transmembrane linker between laminin and actin. *J. Cell Biol.* 122, 809-823.

Félix, R., Serrano, C. J., Treviño, C. L., Muñoz-Garay, C., Bravo, A., Navarro, A., Pacheco, J., Tsutsumi, V. and Darszon, A. (2002). Identification of distinct K<sup>+</sup> channels in mouse spermatogenic cells and sperm. *Zygote* 10, 183-188.

Gee, S. H., Madhavan, R., Levinson, R. S., Caldwell, J. H., Sealock, R. and Froehner, S. C. (1998). Interaction of muscle and brain sodium channels with multiple members of the syntrophin family of dystrophin-associated proteins. *J. Neurosci.* 18, 128-137.

Hernández-González, E. O., Lecona-Valera, A. N., Escobar-Herrera, J. and Mújica, A. (2000). Involvement of an F-actin skeleton on the acrosome reaction in guinea pig spermatozoa. *Cell Motil. Cytoskeleton* 46, 43-58.

Hernández-González, E. O., Martínez-Rojas, D., Mornet, D., Rendón, A. and Mújica, A. (2001). Comparative distribution of short dystrophin superfamily products in various guinea pig spermatozoa domains. *Eur. J. Cell Biol.* 80, 792-798.

Howard, P. L., Klamut, H. J. and Ray, P. N. (1998). Identification of a novel actin binding site within the Dp71 dystrophin isoform. *FEBS Lett.* 441, 337- 341.

Ibraghimov-Beskrovnaya, O., Ervasti, J. M., Leveille, C. J., Slaughter, C. A., Sernett, S. W. and Campbell, K. P. (1992). Primary structure of dystrophin-associated glycoproteins linking dystrophin to the extracellular matrix. *Nature* 355, 676-702.

Juárez-Mosqueda, M. L. and Mújica, A. (1999). A perinuclear theca substructure is formed during epididymal guinea pig sperm maturation and disappears in acrosome reacted cells. *J. Struct. Biol.* 128, 225-236.

Lederfein, D., Yafe, D. and Nudel, U. (1993). A housekeeping type promoter, located in the 3' region of the Duchenne muscular dystrophy gene, controls the expression of Dp71, a major product of the gene. *Hum. Mol. Genet.* 2, 1883-1888.

Loh, N. Y., Nebenius-Oosthuizen, D., Blake, D. J., Smith, A. J. H. and Davies, K. E. (2001). Role of  $\beta$ -dystrobrevin in nonmuscle dystrophin-associated protein complex-like complex in kidney and liver. *Mol. Cell. Biol.* 21, 7442-7448.

Ozaki-Kuroda, K., Nakanishi, H., Ohta, H., Tanaka, H., Kurihara, H., Mueller, S., Irie, K., Ikeda, W., Sakai, T., Wimmer, E., Nishimune, Y. and Takai, Y. (2002). Nectin couples cell-cell adhesion and the actin scaffold at heterotypic testicular junctions. *Curr. Biol.* 12, 1145-1150.

Patrat, C., Serres, C. and Jouannet, P. (2000). Induction of a sodium ion influx by progesterone in human spermatozoa. *Biol. Reprod.* 62, 1380-1386.

Rivier, F., Robert, A., Hugon, G., Bonet-Kerrache, A., Nigro, V., Fehrentz, J. A., Martínez, J. and Mornet, D. (1999). Dystrophin and utrophin complexed with different associated proteins in cardiac Purkinje fibres. *Histochem. J.* 31, 425-432.

Shi, Y. L. and Ma, X. H. (1998). Ion-channels reconstituted into bilayer from human sperm plasma membrane. *Mol. Reprod. Dev.* 50, 354-360.

Tinsley, J. M., Potter, A. C., Phelps, S. R., Fisher, R., Trickett, J. I. and Davies, K. E. (1996). Amelioration of the dystrophic phenotype of mdx mice using a truncated utrophin transgene. *Nature* 384, 349-353.

Trimmer, J. S., Cooperman, S. S., Tomiko, S. A., Zhou, J. Y., Crean, S. M., Boyle, M. B. and Kallen, R. G. (1989). Primary structure and functional expression of a mammalian skeletal muscle sodium channel. *Neuron* 3, 33-49.

Yang, B., Jung, D. J., Rafael, A., Chamberlain, J. S. and Campbell, K. P. (1995). Identification of  $\alpha$ -syntrophin binding to syntrophin triplet, dystrophin, and utrophin. *J. Biol. Chem.* 270, 4975-4978.

Wilson, J., Putt, W., Jimenez, C. and Edwards, Y. E. (1999). Up71 and Up140, two novel transcripts of utrophin that are homologues of short forms of dystrophin. *Hum. Mol. Genet.* 8, 1271-1278.

Winder, S. J. (1997). The membrane-cytoskeleton interface: the role of dystrophin and utrophin. *J. Muscle Res. Cell Motil.* 18, 617-629.